CSIRO PUBLISHING

International Journal of Wildland Fire **2022**, *31*, 56–66
https://doi.org/10.1071/WF21081

Understanding fire regimes in Europe

Luiz Felipe Galizia [A,D], *Thomas Curt* [A], *Renaud Barbero* [A] and *Marcos Rodrigues* [B,C]

[A]INRAE, RECOVER, Aix-Marseille University, Aix-en-Provence, 13182, France.
[B]Department of Agricultural and Forest Engineering, University of Lleida, Lleida, 25198, Spain.
[C]Department of Geography and Land Management, University of Zaragoza, GEOFOREST Group, 50009, Spain.
[D]Corresponding author. Email: luiz.galizia@inrae.fr

Abstract. Wildland fire effects are strongly associated with fire regime characteristics. Here, we developed the first European pyrogeography based on different fire regime components to better understand fire regimes across the continent. We identified four large-scale pyroregions: a non-fire-prone (NFP) pyroregion featuring nominal fire activity across central and northern Europe; a cool-season fire (CSF) pyroregion scattered throughout Europe; a fire-prone (FP) pyroregion extending mostly across southern Europe; and a highly fire-prone (HFP) pyroregion spanning across northern Portugal, Sicily, and western Balkans. Land cover analysis indicates that pyroregions were first shaped by vegetation and then by anthropogenic factors. On interannual timescales the spatial extent of pyroregions was found to vary, with NFP showing more stability. Interannual correlations between climate and burned area, fire frequency, and the length of fire period exhibited distinct patterns, strengthening in fire-prone pyroregions (FP and HFP) and weakening in NFP and CSF. Proportion of cool-season fires and large fires were related to fuel accumulation in fire-prone pyroregions. Overall, our findings indicate that such a pyrogeography should allow a more accurate estimate of the effects of climate on fire regimes while providing an appropriate framework to better understand fire in Europe.

Keywords: pyrogeography, Europe, climate, vegetation, spatial clustering, fire weather index, fire regime, land cover.

Received 9 June 2021, accepted 26 October 2021, published online 23 November 2021

Introduction

Wildland fire is a major hazard throughout Europe, causing extensive economic and ecological impacts (Costa *et al.* 2020; Forzieri *et al.* 2021). These impacts are strongly associated with fire regime components such as the amount of burned area, the frequency of fire ignitions, their intensity, seasonality, or size, and collectively shape the so-called fire regimes (Morgan *et al.* 2001; Bowman *et al.* 2020). Fire regimes are usually defined as the average conditions of the aforementioned components that are persistent and consistent within a particular spatio-temporal unit (Krebs *et al.* 2010). Fire regimes are thus of great interest worldwide, given their potential utility to determine prevailing fire activities and foresee future alterations in response to global change.

Studies dealing with fire at global or continental scales normally use coarse-resolution spatial units, within which fire regime components are aggregated for statistical or modelling purposes. In Europe, these may be administrative units (Turco *et al.* 2017), ecological units (Barbero *et al.* 2019), or a combination of them (Oliveira *et al.* 2014). These classifications may capture to some extent the spatial variability of fire regime components, but their ability to provide an optimal view of fire regimes is, at least, questionable because they assume that fire activity within the target spatial unit is homogenous (Boulanger *et al.* 2012). This is particularly true in Europe where fires occur across a variety of bioclimatic conditions in response to a range of human practices that ultimately drive wildland fires (Adámek *et al.* 2018; Moreira *et al.* 2020; Pinto *et al.* 2020). Likewise, consistent fire regimes across different spatial units may result in artificial segmentations. This spatial diversity is thus hindering our understanding of fire-driving forces from one region to another.

The classification of fire regimes into homogeneous zones is thought to capture the spatial heterogeneity of fire regimes better than existing ecological or political classifications (Boulanger *et al.* 2012). The classification is normally designed through the identification of similar distributions of fire regime components whose spatial extent constitutes the so-called ‘pyroregions’. Such classification provides a level of generalisation that aids in understanding fire regimes at multiple spatial scales (Erni *et al.* 2019) and contributes to improving the performance of statistical models predicting future fire regimes (Flannigan *et al.* 2005; Boulanger *et al.* 2014). Therefore, pyroregions can be seen as a tool towards effective fire risk management and planning (Bowman *et al.* 2013; Fréjaville and Curt 2015).

There are many different methods to delineate pyroregions, either qualitatively or quantitatively. Qualitative approaches rely on expert judgment-based heuristics and have the advantage of integrating multiscale aspects of fire regimes, such as expert and traditional knowledge (Erni *et al.* 2019). However, the lack of transparency and quantitative support has set constraints on their utility (Kreft and Jetz 2010). Quantitative methods aim to reduce subjectivity, relying on empirical data and spatially discrete units (e.g. grid cells) over which fire regime components are aggregated (Boulanger *et al.* 2012). These units are then grouped into several classes using unsupervised learning techniques (e.g. Archibald *et al.* 2013; Chuvieco *et al.* 2008; Rodrigues *et al.* 2020*a*). This approach has been extensively used in global (Chuvieco *et al.* 2008; Archibald *et al.* 2013) and regional analyses (Moreno and Chuvieco 2013; Fréjaville and Curt 2015; Rodrigues *et al.* 2020*b*) but has not been implemented at the European level yet.

A potential limitation of this approach lies in the temporal variability of fire regimes and their drivers. Indeed, pyroregions reflect fire regimes averaged over a given time period, and may be subject to large changes on interannual timescales and over the longer term in response to global change (Bowman *et al.* 2020). These changes may partly relate to atmospheric conditions, one of the main drivers of fire activity across parts of Europe on interannual timescales (Bedia *et al.* 2015; Turco *et al.* 2017; Calheiros *et al.* 2020). Weather and climate control fire regimes by acting respectively on both fuel moisture (direct effect) and fuel accumulation (indirect effect) (Pausas and Keeley 2021). Several studies have demonstrated the influence of fire weather on a range of fire regime components such as occurrence (Ager *et al.* 2014), burned area (Krikken *et al.* 2021), and large fires (Barbero *et al.* 2019), by controlling landscape flammability (e.g. Pellizzaro *et al.* 2007; Pausas and Paula 2012).

In this work, we developed the first European pyrogeography based on different fire regime components to better understand wildland fire activity across the continent. Although most of the pyrogeography studies have focused on the spatial dimension, this study also investigates the temporal dimension and seeks to estimate to what extent climate and fuel drive fire regime components across the pyroregions. We sought to answer the following questions: (1) How fire regime components shape pyroregions across Europe? (2) How vegetation and anthropogenic land cover are distributed throughout pyroregions? (3) How stable are pyroregions on interannual timescales? (4) To what extent climate and fuel accumulation shape fire regime components on interannual timescales? This study may inform the fire community about current fire regimes in Europe and may serve as a basis to simulate future fire regimes on a continental scale.

Methods

Study area

We focused on the European Economic Area (EEA), an area covering a total surface of 4 920 000 km^2. The EEA is very diverse in terms of land cover, vegetation, climate, and human activities. Wildland and agricultural lands are the main land cover type (respectively 39% and 33% of the total area) with most of the fuel load (i.e. burnable surface), whereas urban settlements occupy a small share of the total area (3%) (European Union 2018).

Climate conditions depict a progressive transition from mediterranean climate in the south to subarctic climate in the north. A longitudinal gradient is also seen across the continent featuring a temperate oceanic climate across parts of the west and a more continental climate moving into Eastern Europe. In response to this climatic gradient, vegetation varies from subarid shrublands (i.e. sclerophyllous vegetation and *Pinus halepensis*) in the south to temperate forests (i.e. *Fagus sylvatica* and *Acer pseudoplatanus*) and heather in the centre, and boreal forests (i.e. *Pinus sylvestris*, *Picea abies*, and *Betula spp.*) in the north (San-Miguel-Ayanz *et al.* 2016).

Fire activity generally increases moving southwards, where warm and dry conditions facilitate landscape flammability and fire spread (Turco *et al.* 2017; Forzieri *et al.* 2021). Most fires are due to human-caused ignitions (Ganteaume *et al.* 2013; Adámek *et al.* 2018; Sjöström *et al.* 2019), with most of the total burned area linked to a limited number of large fires occurring during the warm season (Turco *et al.* 2016). Even though lightning-caused fires are comparatively rare in EEA, they may result in large-scale burning and considerable impacts in some regions (Fernandes *et al.* 2021).

Fire data

We used daily fire data from GlobFire (Artés *et al.* 2019), a remotely sensed dataset of individual fires, to assess fire activity over the period 2001–2018. As opposed to gridded burned area products providing the total burned area in a given pixel, datasets of individual fires provide additional information about fire activity, such as the location and spatial extent of each fire from the pixel-based burned area MODIS product MCD64A1 Collection 6 (Giglio *et al.* 2018). We used the GlobFire dataset given its temporal coverage and reasonable agreement with ground-based fire databases across South-western Europe, especially for fires larger than 100 ha (Galizia *et al.* 2021). Note that other remotely sensed datasets of individual fires such as Fire Atlas (Andela *et al.* 2019) and FRY (Laurent *et al.* 2018) show little differences with GlobFire at least in terms of interannual variability (Galizia *et al.* 2021).

We excluded fires located within artificial or agricultural lands because they are generally low intensity, under control, and do not put ecosystems at risk. To do so, we used Corine Land Cover (CLC; European Union 2018) to account for land cover dynamics over the study period. CLC 2000 was used as a reference to filter fires occurring in the 2001–2003 period, CLC 2006 from 2004 to 2009, CLC 2012 from 2010 to 2015, and CLC 2018 from 2016 to 2018. The final dataset was restricted to 78 964 fires, which represents a total burned area of 6 090 696 ha across the study area.

Fire regime components

We aggregated daily fire data onto a 50-km grid cell using the fire patch centroid as a spatial reference to compute five fire regime components (see below). These components were used in previous studies and represent average conditions over the study period in terms of fire incidence, seasonality, and size distribution (Chuvieco *et al.* 2008; Archibald *et al.* 2013; Curt *et al.* 2014; Rodrigues *et al.* 2020*b*). This resolution seeks to capture the local variation in the fire regime, while gathering enough fires in each grid cell for statistical purposes. We omitted fire data in grid cells where more than 80% of the surface was non-burnable (i.e. anthropogenic lands), following Abatzoglou *et al.* (2019).

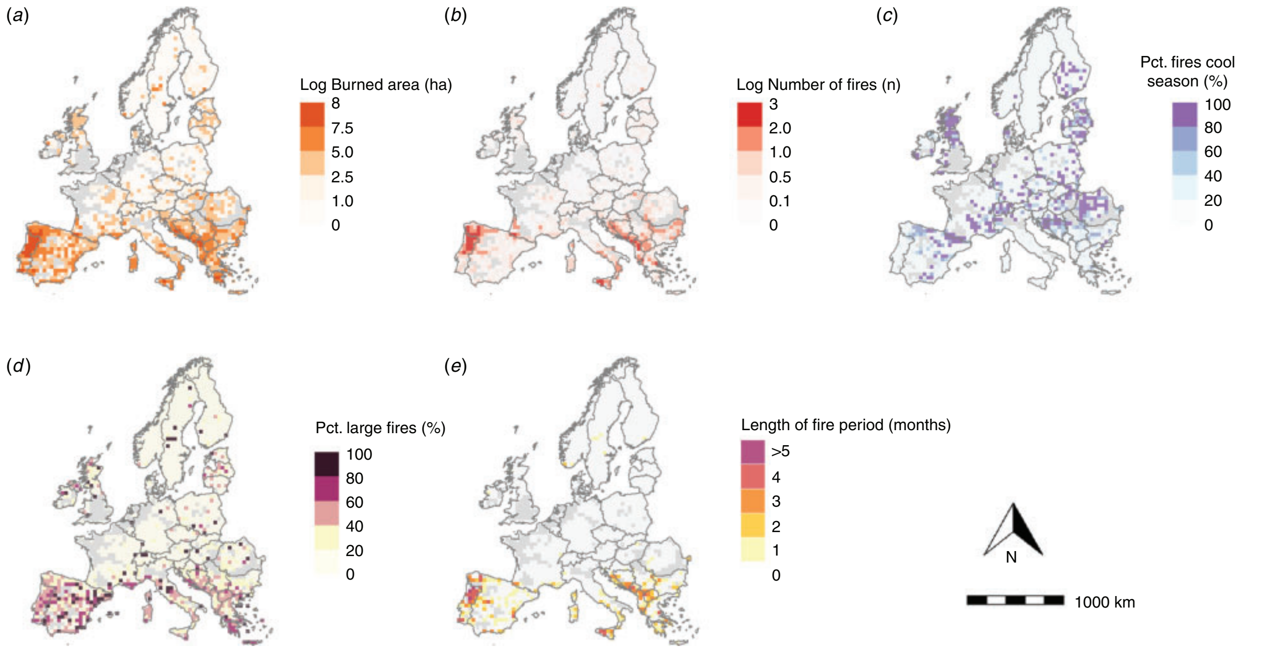

Fig. 1. The five fire regime components include (*a*) the mean annual burned area, (*b*) the mean annual number of fires, (*c*) the percentage of fires taking place during the cool season (November–April), (*d*) the percentage of large fires (>100 ha), and (*e*) the mean length of fire period. Regions with more than 80% of non-burnable land cover are shaded dark grey.

Mean annual burned area (BA; ha yr^{-1})

This metric was derived as a general indicator of fire hazard (Fig. 1*a*). The BA was defined as:

$$BA_{xy} = \frac{\sum BAd_{xy}}{k} \tag{1}$$

where *BA* is the sum of daily burned area *BAd* in the grid cell *xy*, divided by the total number of years *k*.

Mean annual number of fires (NF; n yr^{-1})

This metric was derived as a general indicator of fire occurrence, regardless of their spatial extent (Fig. 1*b*). The NF was defined as:

$$NF_{xy} = \frac{\sum NFd_{xy}}{k} \tag{2}$$

where *NF* is the total number of fires *NFd* in the grid cell *xy*, divided by the total number of years *k*.

Percentage of fires during the cool season (PFCS; %)

This was defined as the rate of fire events occurring during the November–April period (Fig. 1*c*). This metric was derived as a general indicator of fire seasonality and fire type (i.e. agricultural and prescribed burnings generally take place in the winter (November–February) or early spring (March–April)). The PFCS was defined as:

$$PFCS_{xy} = \frac{\sum NFCS_{xy}}{\sum NF_{xy}} \times 100 \tag{3}$$

where *NFCS* is the total number of fires during the cool season in the grid cell *xy*, divided by the total number of fire events in the grid cell *xy*.

Percentage of large fires events (PLF; %)

This was defined as the percentage of fire events larger than 100 ha (Fig. 1*d*). This metric was derived as a general indicator of fire size distribution. The PLF was defined as:

$$PLF_{xy} = \frac{\sum NLF_{xy}}{\sum NF_{xy}} \times 100 \tag{4}$$

where *NLF* is the total number of large fires events in the grid cell *xy*, divided by the total number of fire events in the grid cell *xy*.

Mean length of fire period (LFP; months)

This was defined as the number of calendar months in the year during which the mean monthly burned area exceeded 100 ha (Fig. 1*e*). This metric was derived as a general indicator of the length of the fire-prone window (LBA). The LFP was defined as:

$$LFP_{xy} = \sum LBA_i \tag{5}$$

where $LBA_m = 1$ if $MBA_{m,xy} > 100$; otherwise $LBA_m = 0$. *MBA* is the mean burned area by month *m*, in the grid cell *xy*.

Delineating pyroregions

We delineated the European pyroregions based on the aforementioned fire regime components reflecting the average conditions of fire activity at the grid cell level over the period 2001–2018 (Fig. 1). Pyroregions were built through a hierarchical cluster analysis (Ward 1963). Hierarchical clustering has been widely used in fire science (Boulanger *et al.* 2012; Jiménez-Ruano *et al.* 2020; Rodrigues *et al.* 2020*b*) because it has the advantage of not requiring *a priori* information about the number of clusters. Fire regime components were rescaled into *Z*-scores with a zero mean and a unit variance, as recommended in most clustering approaches. The clustering strategy consisted of Euclidean distance as dissimilarity measure and Ward's minimum variance method *ward.D2*, which minimises the inter-cluster variance (Sørensen 1948). The optimal number of clusters was determined using the highest-ranked number of clusters out of 30 indices available in the *nbClust* R package (Charrad *et al.* 2014). The resulting clusters were considered representative of the pyroregions.

We then tested the stability of our clustering analysis to the spatial sampling. To do so, we randomly resampled 70% of the fire regime components across Europe and compared the clustering based on this subsample with the pyroregions obtained from the initial classification based on the whole sample. The agreement between both classifications was estimated through the mean accuracy (i.e. proportion of agreement) and the Kappa Cohen's index (Cohen 1960). The process was repeated 1000 times to ensure the consistency of agreement measurements (Rodrigues *et al.* 2020*b*).

Interannual stability of the pyrogeography

Because fire regime components are likely to change with time, we investigated the interannual stability of our pyrogeography over the studied period by recomputing all fire regime components on a yearly basis. We then used the k-nearest neighbour classification (KNN; Ripley 1996) to replicate our pyrogeography at an annual timescale. KNN is a supervised nonparametric classifier that assigns a category (i.e. pyroregion) according to the similarity/dissimilarity (Euclidean distance, as in the original cluster classification) in an N-dimensional space, where N equals the number of features characterising each observation, i.e. our five fire regime components. The assigned class in KNN is the most frequently observed among the K ($K = 5$) neighbours. We applied the KNN procedure to each grid cell and year, using annualised values of fire regime components (e.g. the number of fires in a given year). We then estimated the interannual stability of pyroregions (ISP; %) by computing the percentage of annual agreement between annualised pyroregions (PRs) and pyroregions based on long-term averages. The ISP was defined as:

$$ISP_{xy} = \frac{\sum N_{yr,xy}}{k} \times 100 \tag{6}$$

where $N_{yr,xy} = 1$ if $PR_{yr,xy} = PR_{xy}$; otherwise $N_{yr,xy} = 0$.

N is an indicator of whether the annualised PR_{yr} classification agreed with the *PR* classification based on long-term averages in the year *yr* at grid cell *xy* divided by the total number of years *k*.

Land cover distribution

Land cover is one of the factors that influence fire regimes at the landscape level. We investigated the distribution of land cover classes across the pyroregions using Corine land cover (European Union 2018). Land cover distribution was calculated as the percentage area of the grid cell (50 km) covered by specific vegetation and anthropogenic land cover (Table 1). We computed land cover distribution averaging the Corine dataset (2000, 2006, 2012 and 2018) over the study period to account for land cover changes through time. Finally, we tested the significance of differences in the distribution of the vegetation and human activities among the pyroregions by means of the non-parametric Wilcoxon signed-rank test.

Fire weather data

We used daily indices from the Canadian Forest Fire Danger Rating System (Van Wagner 1987) to assess the influence of fire weather on fire regime components. Those indices have already been shown to correlate with fire activity globally (Bedia *et al.* 2015; Abatzoglou *et al.* 2018; Wang *et al.* 2020), including across parts of Europe (Barbero *et al.* 2019; Rodrigues *et al.* 2020*a*; Dupuy *et al.* 2020; Ruffault *et al.* 2020). We retrieved the daily fine fuel moisture code (FFMC), the duff moisture code (DMC), the drought code (DC), the daily initial spread index (ISI), the accumulation index (BUI), and the fire weather index (FWI) from the Copernicus Climate Change Service (C3S; https://climate.copernicus.edu) at 25-km resolution from the period 2001–2018 (Vitolo *et al.* 2020). We then regridded the data onto a 50-km resolution grid to facilitate the comparison with the pyrogeography. Note that the initial starting of soil and fuel moisture indices (FFMC, DMC, and DC) were computed with default values (Vitolo *et al.* 2020).

Vegetation productivity data

We used the net primary production (NPP) of the vegetation as a proxy of fuel availability. Fuel amount during the previous

Table 1. Description of the land cover classes used in the distribution analysis

Maps of the vegetation cover and anthropogenic variables are shown in Figs S2 and S3 (Supplementary Material)

Group	Name	Denotation	Description
Human	Wildland agriculture interfaces	WAI	Percentage of the boundary between agriculture and wildlands land cover classes in the grid cells
	Urban area	Urb	Percentage of urban land in the grid cells
Vegetation	Coniferous forest	Conif	Percentage of coniferous forest in the grid cells
	Broadleaf forest	Broad	Percentage of broadleaf forest in the grid cells
	Mixed forest	Mixed	Percentage of mixed forest in the grid cells
	Shrublands	Shrub	Percentage of shrublands forest in the grid cells

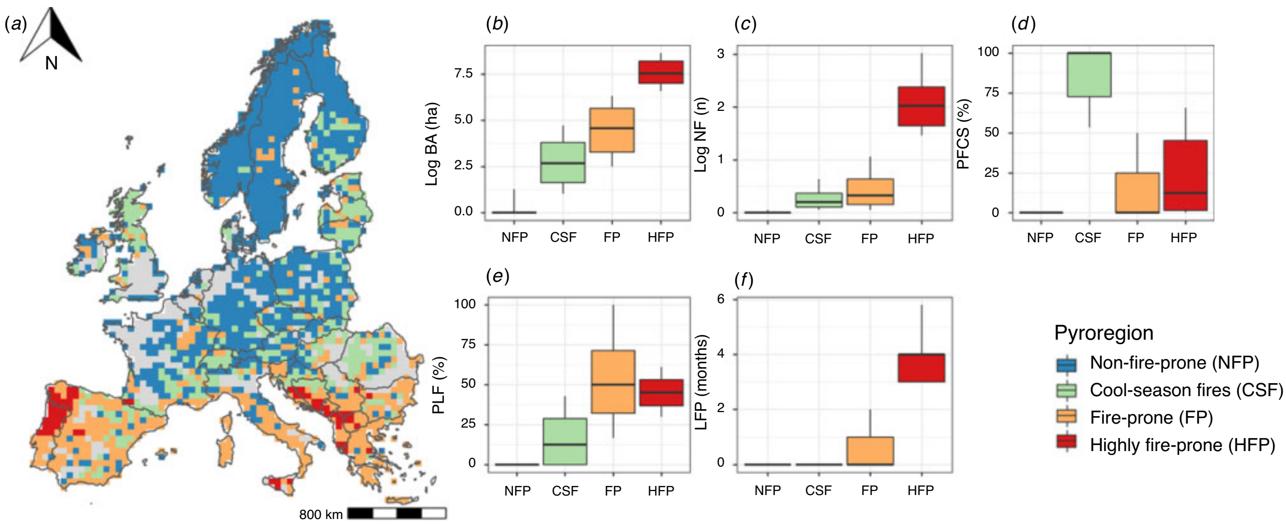

Fig. 2. Spatial distribution of pyroregions and fire regime components distribution (i.e. median and interquartile range) observed in each pyroregion. Regions with more than 80% of non-burnable land cover are shaded grey.

growing season may facilitate fire activity in fuel-limited landscapes (Abatzoglou *et al.* 2018; Archibald *et al.* 2018). We extracted yearly NPP from the Moderate Resolution Imaging Spectroradiometer (MOD17A3; https://lpdaac.usgs.gov/) at 500-m resolution from the period 2000–2018. We then regridded this information onto a 50-km resolution grid for comparison with the pyrogeography.

Interannual climate–fire and productivity–fire relationships

We used annual averages of fire weather indices as indicators of fire danger (Bedia *et al.* 2015; Abatzoglou *et al.* 2018) and NPP as a proxy of fuel accumulation to investigate to what extent climate and fuel shapes fire regime components throughout pyroregions. We spatially aggregated (averaged) annualised fire regime components, fire weather indices, and antecedent vegetation productivity (NPP_{1year}) at the pyroregional scale. Annualised BA and NF were log-transformed to follow a normal distribution. We then computed Pearson's correlation to measure the strength of the concurrent climate–fire relationship as well as the lagged productivity–fire relationship at the pyroregion level. We also aggregated annualised fire features, fire weather, and antecedent productivity over the whole domain (i.e. averaging the data across the study area) to compute the global correlation for comparison with pyroregions.

Results

Delineating pyroregions

We identified four pyroregions with homogeneous fire regime components across Europe (Fig. 2). Cross-correlations between fire regimes components at the pyroregional level are shown in Fig. S4 (Supplementary Material). There was a strong north–south dichotomy in the spatial distribution of pyroregions. A non-fire-prone pyroregion (hereafter NFP) with very low fire activity was found across central and northern Europe. A cool-season fires pyroregion (hereafter CSF) featuring intermediate fire activity with a large percentage of fires occurring during the November–April period was seen across various regions of Europe, including the Alps, parts of the Pyrenees, Scotland, and Romania. Further south, a fire-prone pyroregion (hereafter FP) with high fire activity and a substantial contribution of large fire events to the total burned area was identified across most of Spain, Southern Portugal, Italy, south-east France, and parts of the Balkans. Finally, a highly fire-prone pyroregion (hereafter HFP) featuring the highest fire occurrence, the highest burned area, and the longest fire period length encapsulated the north-western part of Iberian Peninsula, Sicily, Adriatic, and part of the Balkans. Note that both FP and HPF presented a considerable percentage of fires occurring in the cool season (>10%), suggesting a bimodal fire season as seen in some regional analyses (e.g. Pimont *et al.* 2021). Our classification was relatively insensitive to the spatial resampling with an average accuracy of 80% and a Kappa index of 0.7.

The NFP was the largest pyroregion (2 140 000 km^2) covering 50.6% of burnable grid cells (Table 2). The FP (1 092 500 km^2) and the CSF (837 500 km^2) were comparatively smaller, with respectively 25.8% and 19.8% of the grid cells. The HPF was the smallest (157 500 km^2), with 3.7% of the grid cells, but accounted for most of the fire activity (i.e. 89.6% of total burned area and 88.1% of total number of fires).

Interannual stability of the pyrogeography

On interannual timescales, pyroregions presented different rates of ISP, with the NFP showing the longest persistence over the period, followed by FP, HFP, and CSF (Fig. 3*a*). Fig. 3*b* shows the spatial distribution of ISP. Overall, we found higher stability (ISP >60%) in central-northern Europe, in western Iberian Peninsula, as well as in Sardinia, parts of Italy, and the Balkans. In contrast, lower stability (ISP <20%) was found in specific regions such as in northern UK, across mountainous regions in central Europe, and the Baltics.

Land cover distribution

We found contrasting distributions of land cover classes across the pyroregions (Fig. 4). Overall, vegetation classes displayed

Table 2. Summary of pyroregions features

Area, spatial extent; BA, mean annual burned area; NF, mean annual number of fires; PLF, percentage of large fires; PFCS, percentage fire during the cool season; LFP, length of fire period. Fire regime components values indicate the spatial mean and the relative contribution (in %) to the European domain respectively

Pyroregion	Area (km^2)		BA (ha)		NF (n)		PLF (%)		PFCS (%)		LFP (m)	
Highly fire-prone	157 500.0	3.7%	2634.2	89.6%	8.7	88.1%	44.5	39.3%	25.9	20.2%	4.0	87.2%
Fire-prone	1 092 500.0	25.8%	264.5	9.0%	0.8	7.7%	52.7	46.6%	15.8	12.3%	0.5	10.9%
Cool-season fire	837 500.0	19.8%	41.7	1.4%	0.4	3.9%	16.0	14.1%	86.5	67.5%	0.1	1.9%
Non-fire-prone	2 140 000.0	50.6%	0.7	0.0%	0.0	0.2%	–	0.0%	–	0.0%	–	0.0%

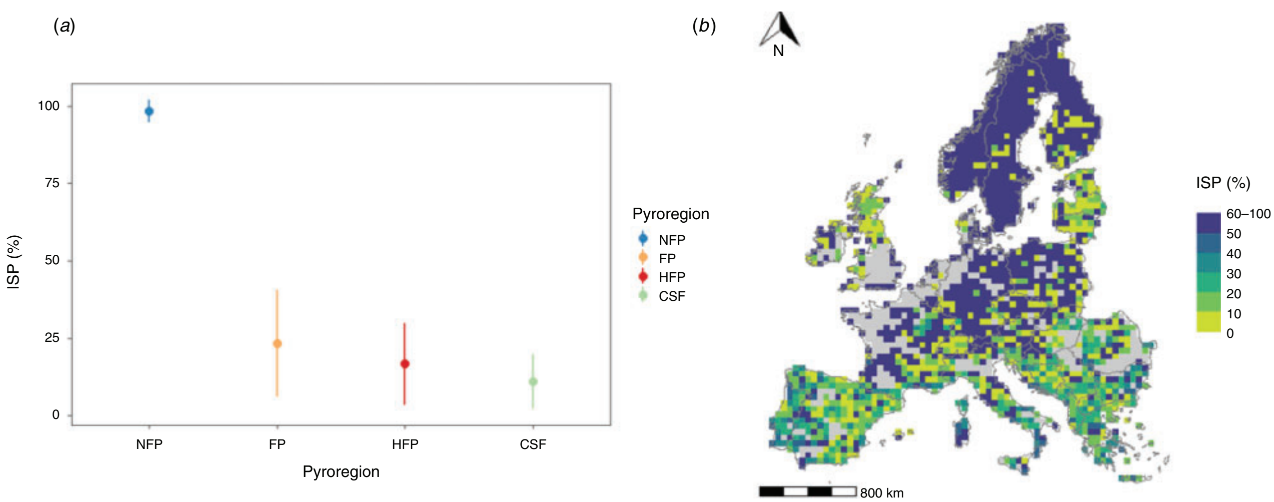

Fig. 3. (*a*) Distribution (i.e. mean and standard deviation range) of the interannual stability of pyrogeography (ISP) and (*b*) the ISP at grid cell level. ISP is computed as the percentage of annual agreement between annualised pyroregions and pyroregions based on long-term averages in the study period.

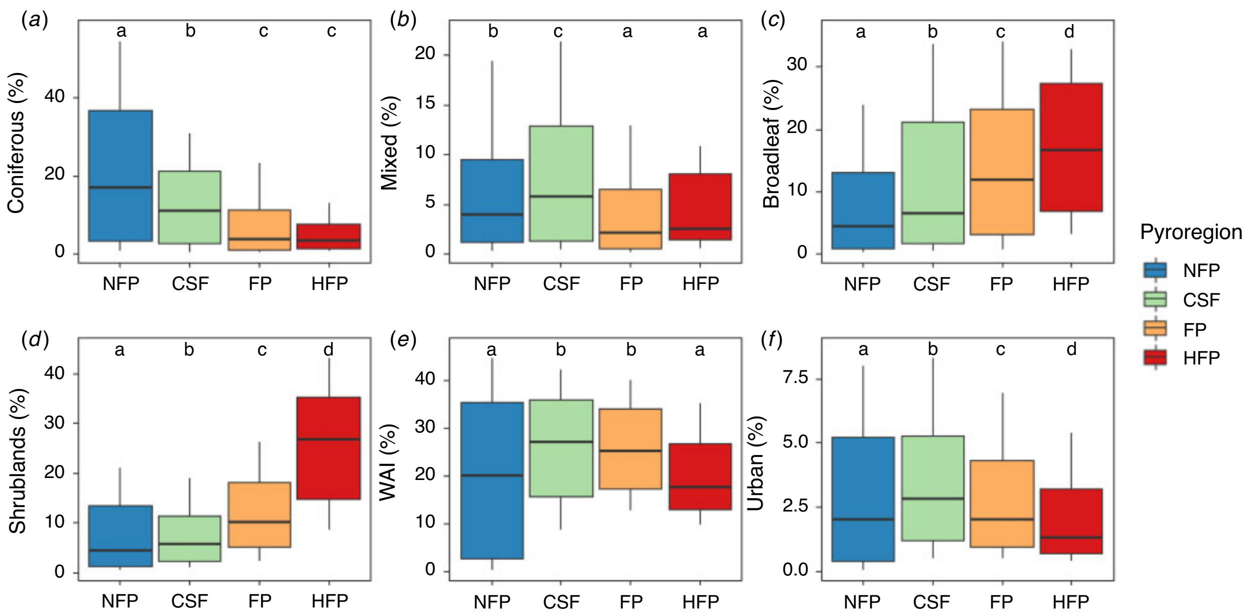

Fig. 4. Land cover distribution of (*a–d*) vegetation and (*e*, *f*) anthropogenic variables across the pyroregions. Lines represent the median and interquartile range of the data. Significantly different distributions (Wilcoxon signed-rank test) are indicated with different letters.

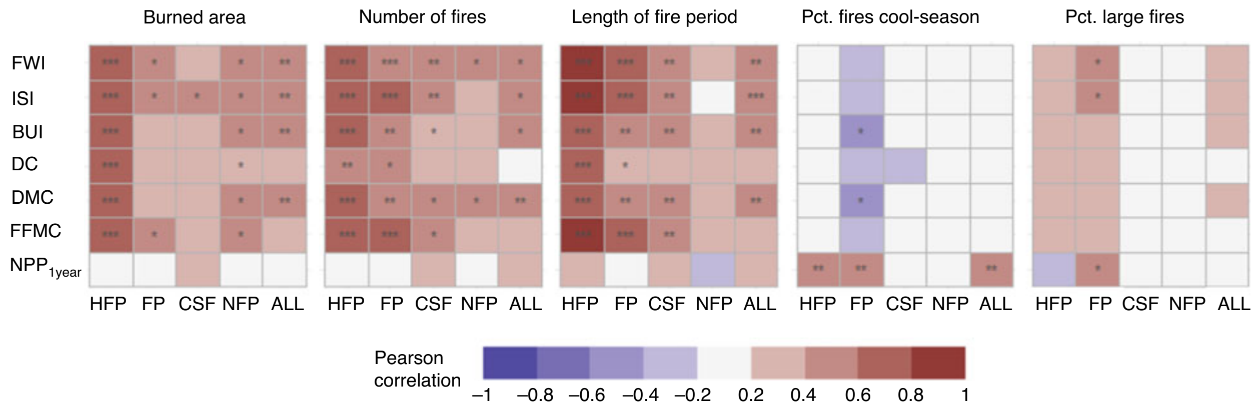

Fig. 5. Interannual relationships between fire regime components (from left to right) and fire weather indices, and antecedent net primary productivity (*y*-labels) in each pyroregion (*x*-labels), as well as aggregated over the whole domain (ALL). Symbols represent the significance level (*** for $P < 0.01$; ** for $P < 0.05$; * for $P < 0.1$).

larger differences between pyroregions than anthropogenic did, indicating that pyroregions occurrence is likely first mediated by vegetation. Specifically, the large proportion of shrublands in HFP is evidencing the high fire proneness of this vegetation type (Ganteaume *et al.* 2013; Oliveira *et al.* 2014). Conversely, coniferous and mixed forests dominate NPF and CSF, respectively. The wildland agricultural interfaces presented higher incidence in CSF and FP regions, with CSF showing also higher urban areas, highlighting the human pressure on wildlands into these regions.

Interannual climate–fire and productivity–fire relationships

Climate–fire correlations exhibited distinct patterns across the pyroregions (Fig. 5). Overall, positive correlations between fire weather indices and fire regime components were the highest in pyroregions with higher fire activity. Burned area presented strong positive correlations (>0.6) with all fire weather indices in the HPF pyroregion and moderate correlations (>0.4) in other pyroregions. Number of fires and length of fire period presented strong positive correlations (>0.6) as well with the majority of fire weather indices in most of pyroregions, except for NFP. Specifically, length of fire period presented the highest correlations with FWI, ISI, and FFMC in both FP and HFP pyroregions. Also, the percentage of large fires showed a moderate correlation (>0.4) with FWI and ISI in the FP pyroregion. Conversely, the percentage of fires during the cool season presented weak negative correlations with DMC and BUI in the FP pyroregion. Regarding the indirect effect of antecedent conditions, the NPP_{1year} attained moderate correlations (>0.4) with the percentage of fires during the cool season in HPF and FP pyroregions, and with the percentage of large fires in FP. Note that pooling all pyroregions together (ALL) degraded the climate–fire relationships detected in fire-prone pyroregions.

Discussion

Wildland fire risk management calls for efficient approaches to better understand fire activity at different spatio-temporal scales (Johnston *et al.* 2020; Taylor 2020). Grouping regions with similar fire regime components may help develop efficient strategies to manage fires across broad scales and to aggregate data over regions with consistent fire regimes (Boulanger *et al.* 2012; Curt *et al.* 2014). Here, we sought to synthesise a range of fire regime components to build the first European pyrogeography.

Four pyroregions were considered representative of the pan-European fire regime with contrasted patterns of fire activity (Fig. 2 and Fig. S4, Supplementary Material). The non-fire-prone pyroregion (NFP) was the largest (≈50% of the whole domain), representing a small part of fire events (<1%). Conversely, fire-prone pyroregions (FP and HFP) covered a small part of burnable grid cells (≈30%), but accounted for most of the fire events occurring during the warm season (>80%). Finally, a cool-season fires pyroregion (CSF) reflected mostly intentional burning related to traditional pastoral practices across Europe in winter or early spring. Overall, CSF presented less spatial continuity than the other pyroregions, mainly due to the influence of human-related activities, such as agriculture and pastoral activities. This pyrogeography partly resembled that from previous regional studies in Southern Europe (Moreno and Chuvieco 2013; Silva *et al.* 2019; Rodrigues *et al.* 2020*b*).

On shorter timescales, pyroregions may change, switching from one category to another. Identifying regions featuring persistent fire regimes across Europe may support wildland fire suppression capacity, surveillance, and resources allocation at a broad scale (Taylor 2020). This may also enable the assessment of fire deficits over time across the pyroregions, ultimately helping devising fuel treatment campaigns. By examining the sensitivity of our classification to the interannual variability of fire regime components, we also quantify the uncertainty of our classification while understanding how pyroregions may change in the future (Cochrane and Bowman 2021). This is paramount from a fire risk management perspective because decisions are taken at many different scales (Parisien *et al.* 2014; Taylor 2020).

Our analysis also indicates that fire regimes stem, to some extent, from the type of fuels present in a particular ecosystem (Fig. 4). Conversely, the distribution of human factors displayed less variability among the pyroregions, indicating lower agreement with the pyrogeography. In CSF and FP only, human activities play a similar role to vegetation in determining current pyroregions. However, we must stress that such broad-scale pyroregions are driven by complex interactions (i.e. climate, ignition, and vegetation), and each fire regime component may respond to specific ecological conditions at many different spatial scales (Parisien and Moritz 2009; Duane and Brotons 2018; Ruffault *et al.* 2020). For instance, vegetation features such as species, density, and fuel structure influence fire activity locally, but remain hidden in broad-scale analyses (Pellizzaro *et al.* 2007; Harris *et al.* 2016).

Interannual climate–fire relationships exhibited patterns in line with those reported in regional (Venäläinen *et al.* 2013; Jiménez-Ruano *et al.* 2019) and global studies (Bedia *et al.* 2015; Abatzoglou *et al.* 2018). Positive correlations between fire weather indices and most fire regime components (burned area, number of fires, and length of fire period) strengthened in pyroregions with higher fire activity (Fig. 5). Specifically, our study highlights the influence of climate in controlling the length of the fire-prone window across the pyroregions (Pausas and Keeley 2021). The higher correlation found in the number of fires compared with burned area may indicate that burned area is influenced by a few random large fires that deteriorate the climate–fire relationship (Pimont *et al.* 2021). Positive correlations between fire weather indices and fire regime components emphasise the importance of annual fire weather conditions in enabling fire activity across fire-prone pyroregions (Williams *et al.* 2015; Abatzoglou *et al.* 2018). However, among fire-prone pyroregions climate–fire correlations may also weaken as the fire danger increases and the productivity of vegetation decreases (Fig. S5, Supplementary Material), where fuel abundance may be a limiting factor (Abatzoglou *et al.* 2018; Pausas and Keeley 2021). Weaker correlations found in CSF and NFP might be related to the overall high level of fuel moisture content, which does not decrease sufficiently throughout the years to allow fire spread. Other factors besides climate may also degrade the climate–fire relationships in these pyroregions, such as lack of fuel continuity, high fire-fighting capability, or low ignition potential (Abatzoglou *et al.* 2018; Pausas and Keeley 2021). Finally, climate was found not to be related to percentage of fires during the cool season and percentage of large fires in all pyroregions, indicating that other drivers may better explain their interannual variability.

Fuel accumulation can be relevant in driving fire in some pyroregions (Pausas and Ribeiro 2013). Negative correlation between percentage of fires during the cool season and two fire weather indices (BUI and DMC) in the FP pyroregion may reflect the effects of fuel accumulation during wet years. Previous research has shown that climate during the precedent growing season may influence vegetation productivity and ultimately fire activity (Yin *et al.* 2020; Rodrigues *et al.* 2021). Positive correlations between the antecedent net primary productivity and the percentage of fires during the cool season in HPF and FP pyroregions indicate increased burning due to fuel accumulation over the previous year (Fernandes *et al.* 2014). Likewise, positive correlations between the antecedent net primary productivity and percentage of large fires in FP pyroregions indicates an increase in the proportion of large fires fostered by fuel accumulation. This is consistent with fuel-limited fire regimes in dry and warm ecoregions (Abatzoglou *et al.* 2018; Pausas and Keeley 2021). Yet, the antecedent net primary productivity did not show significant correlations with burned area and number of fires.

By aggregating fire regime components, fire weather indices and antecedent vegetation productivity at pyroregions, we presented more consistent relationships; these regions better captured the spatial heterogeneity of the fire regime components than existing political (Calheiros *et al.* 2020) or ecological classifications (Boulanger *et al.* 2012; Abatzoglou *et al.* 2018). Specifically, the strong climate–fire relationships found here indicate that pyroregions should allow for more precise spatially explicit modelling of the effects of climate on fire regimes across broad scales. They may also help outline future areas with high fire risk while providing an appropriate framework for wildland fire management (Boulanger *et al.* 2014; Jiménez-Ruano *et al.* 2020). However, we acknowledge that our stratification is likely, as with any other stratification, to mix up fires with different human causes and fuel types. Also, despite the overall strong relationship found here, it is noted that fire activity is unlikely to be unilaterally responsive to climate (Archibald *et al.* 2013; Fréjaville and Curt 2017; Jiménez-Ruano *et al.* 2019) and fuel accumulation (Moreira *et al.* 2020), but driven by interactions among climate, vegetation, and human activities (Bowman *et al.* 2020; Pausas and Keeley 2021; Cochrane and Bowman 2021). Also, further analysis on fire ecology (e.g. mortality, vegetation recovery rates, or species composition) at a finer scale will help to clarify the links between vegetation and fire regimes. Similarly, evaluating human factors that directly or indirectly relate to fire ignitions may provide valuable insights into the role of human activities in shaping these pyroregions.

Our pyrogeography offers a meaningful segmentation of fire regimes across Europe, which may serve as a basis to model the effects of global change on fire in Europe. We are aware that fire regimes can be described by additional variables, including driving variables such as vegetation or climate into the classification. However, the selection of variables depends on the objectives (Krebs *et al.* 2010; Bowman *et al.* 2013). Here, our aim is to characterise the fire regime focusing on fire regime components only. Including fire drivers into the classification may improve the spatial continuity of the pyroregions, due to their spatial autocorrelation, but may also degrade the fire regime characterisation. We chose these components because they are frequently used in pyrogeography and describe key aspects of fire regimes (Boulanger *et al.* 2012; Jiménez-Ruano *et al.* 2020; Rodrigues *et al.* 2020*b*). Future work including other attributes that were not available in the remotely sensed dataset of individual fires, such as fire intensity, burn severity, or focusing on detailed analyses of fire seasonality, would add further insights into the characterisation of pyroregions. Additionally, our pyrogeography can be further refined at other subscales depending on the specific needs of the end user.

Remotely sensed fire data used here are relatively short (18 years) when compared with studies using ground-based fire datasets (Boulanger *et al.* 2012; Moreno and Chuvieco 2013; Curt *et al.* 2014). We acknowledge that the use of a longer time period may better capture extreme fire seasons with longer return periods. Also, the overall low capacity of remote-sensing products to detect small-sized fires (<100 ha) may underestimate fire frequency (Roteta *et al.* 2019; Galizia *et al.*

2021). However, remote sensing is the only source of homogeneous and harmonised data covering the whole European continent, and has been shown to capture very well the temporal variability in fire frequency and burned area (Earl and Simmonds 2018; Turco *et al.* 2019; Galizia *et al.* 2021). Although the data span was too short to identify systematic trends, we acknowledge that substantial changes are likely to occur under future climate and vegetation conditions (Bowman *et al.* 2020; Fargeon *et al.* 2020; Cochrane and Bowman 2021). In this regard, our pyrogeography provides a baseline to understand how fire activity might change and how pyroregions are likely to shrink or expand in the future under global change (Jiménez-Ruano *et al.* 2020; Calheiros *et al.* 2021).

Conclusion

In this work, we developed the first European pyrogeography based on different fire regime components. We additionally examined to what extent climate and fuel accumulation shape fire regime components throughout the pyroregions. Overall, four large-scale pyroregions were considered representative of the pan-European fire regime with different patterns of fire activity across the continent.

Pyroregions occurrence was first mediated by vegetation cover, and then anthropogenic factors, indicating that fire regimes stem, to some extent, from the type of fuels present in a particular ecosystem. On interannual timescales the extent of pyroregions was found to vary, with zones of lower fire activity showing more stability. Interannual climate–fire relationships indicate different effects of fire weather in fire regime components throughout the pyroregions. We reported on strong relationships among fire weather conditions and burned area, number of fires, and the length of the fire period across fire-prone pyroregions (FP and HFP). By contrast, other fire features such as proportion of cool-season fires and large fires were related to fuel accumulation. These results may be informative for identifying which fire features may exhibit substantial changes in the coming decades due to future climate conditions and where they may occur.

Our findings also indicate that such a pyrogeography should allow a more spatially explicit modelling of the effects of climate on fire regimes. Additionally, this may also provide a baseline to understand how fire activity might change in response to global change. In this regard, further studies are still needed to evaluate future changes in the distribution of pyroregions in order to support wildland fire risk management across the European domain.

Data availability statement

All the data that support this study are open access and can be accessed using websites or data repositories described below. Remotely sensed fire dataset is available at https://doi.pangaea.de/10.1594/PANGAEA.895835 (Artés *et al.* 2019). The ERA5 high-resolution reanalysis of the Canadian FWI System indices are available at https://climate.copernicus.edu (Vitolo *et al.* 2020). Land cover dataset is available at https://land.copernicus.eu/pan-european/corine-land-cover. Vegetation productivity data is available at https://lpdaac.usgs.gov/.

Conflicts of interest

The authors declare no conflicts of interest.

Declaration of funding

This work was funded by project MED-Star, supported by the European Union under the Operational Program Italy/France Maritime (project number CUP E88H19000120007). Marcos Rodrigues has received funding from the European Union's Horizon 2020 research and innovation programme under grant agreement No 101003890, FirEUrisk – DEVELOPING A HOLISTIC, RISK-WISE STRATEGY FOR EUROPEAN WILDFIRE MANAGEMENT.

Acknowledgements

The authors thank Vincent Moron and Julien Ruffault for their helpful comments during the early stages of this work.

References

Abatzoglou JT, Williams AP, Boschetti L, Zubkova M, Kolden CA (2018) Global patterns of interannual climate–fire relationships. *Global Change Biology* **24**, 5164–5175. doi:10.1111/GCB.14405

Abatzoglou JT, Williams AP, Barbero R (2019) Global Emergence of Anthropogenic Climate Change in Fire Weather Indices. *Geophysical Research Letters* **46**, 326–336. doi:10.1029/2018GL080959

Adámek M, Jankovská Z, Hadincová V, Kula E, Wild J (2018) Drivers of forest fire occurrence in the cultural landscape of Central Europe. *Landscape Ecology* **15**, 2031–2045. doi:10.1007/S10980-018-0712-2

Ager AA, Preisler HK, Arca B, Spano D, Salis M (2014) Wildfire risk estimation in the Mediterranean area. *Environmetrics* **25**, 384–396. doi:10.1002/ENV.2269

Andela N, Morton DC, Giglio L, Paugam R, Chen Y, Hantson S, van der Werf GR, Randerson JT (2019) The Global Fire Atlas of individual fire size, duration, speed and direction. *Earth System Science Data* **11**, 529–552. doi:10.5194/essd-11-529-2019

Archibald S, Lehmann CER, Gomez-Dans JL, Bradstock RA (2013) Defining pyromes and global syndromes of fire regimes. *Proceedings of the National Academy of Sciences of the United States of America* **110**, 6442–6447. doi:10.1073/PNAS.1211466110

Archibald S, Lehmann CER, Belcher CM, Bond WJ, Bradstock RA, Daniau A-L, Dexter KG, Forrestel EJ, Greve M, He T, Higgins SI, Hoffmann WA, Lamont BB, McGlinn DJ, Moncrieff GR, Osborne CP, Pausas JG, Price O, Ripley BS, Rogers BM, Schwilk DW, Simon MF, Turetsky MR, Van der Werf GR, Zanne AE (2018) Biological and geophysical feedbacks with fire in the Earth system. *Environmental Research Letters* **13**, 033003. doi:10.1088/1748-9326/AA9EAD

Artés T, Oom D, de Rigo D, Durrant TH, Maianti P, Libertà G, San-Miguel-Ayanz J (2019) A global wildfire dataset for the analysis of fire regimes and fire behaviour. *Scientific Data* **6**, 296. doi:10.1038/S41597-019-0312-2

Barbero R, Curt T, Ganteaume A, Maillé E, Jappiot M, Bellet A (2019) Simulating the effects of weather and climate on large wildfires in France. *Natural Hazards and Earth System Sciences* **19**, 441–454. doi:10.5194/NHESS-19-441-2019

Bedia J, Herrera S, Gutiérrez JM, Benali A, Brands S, Mota B, Moreno JM (2015) Global patterns in the sensitivity of burned area to fire-weather: implications for climate change. *Agricultural and Forest Meteorology* **214–215**, 369–379. doi:10.1016/J.AGRFORMET.2015.09.002

Boulanger Y, Gauthier S, Burton Philip J, Vaillancourt M-A (2012) An alternative fire regime zonation for Canada. *International Journal of Wildland Fire* **21**, 1052–1064. doi:10.1071/WF11073

Boulanger Y, Gauthier S, Burton PJ (2014) A refinement of models projecting future Canadian fire regimes using homogeneous fire regime zones. *Canadian Journal of Forest Research* **44**, 365–376. doi:10.1139/CJFR-2013-0372

Bowman DMJS, O'Brien JA, Goldammer JG (2013) Pyrogeography and the global quest for sustainable fire management. *Annual Review of Environment and Resources* **38**, 57–80. doi:10.1146/ANNUREV-ENVIRON-082212-134049

Bowman DM, Kolden CA, Abatzoglou JT, Johnston FH, van der Werf GR, Flannigan M (2020) Vegetation fires in the Anthropocene. *Nature Reviews Earth & Environment* **1**, 500–515. doi:10.1038/S43017-020-0085-3

Calheiros T, Nunes JP, Pereira MG (2020) Recent evolution of spatial and temporal patterns of burnt areas and fire weather risk in the Iberian Peninsula. *Agricultural and Forest Meteorology* **287**, 107923. doi:10.1016/J.AGRFORMET.2020.107923

Calheiros T, Pereira MG, Nunes JP (2021) Assessing impacts of future climate change on extreme fire weather and pyro-regions in Iberian Peninsula. *The Science of the Total Environment* **754**, 142233. doi:10.1016/J.SCITOTENV.2020.142233

Charrad M, Ghazzali N, Boiteau V, Niknafs A (2014) NbClust: an R package for determining the relevant number of clusters in a data set. *Journal of Statistical Software* **61**, 36. doi:10.18637/JSS.V061.I06

Chuvieco E, Giglio L, Justice C (2008) Global characterization of fire activity: toward defining fire regimes from Earth observation data. *Global Change Biology* **14**, 1488–1502. doi:10.1111/J.1365-2486.2008.01585.X

Cochrane MA, Bowman DMJS (2021) Manage fire regimes, not fires. *Nature Geoscience* **14**, 455–457. doi:10.1038/S41561-021-00791-4

Cohen J (1960) A coefficient of agreement for nominal scales. *Educational and Psychological Measurement* **20**, 37–46. doi:10.1177/001316446002000104

Costa H, Rigo D, Libertà G, Houston Durrant T, San-Miguel-Ayanz J (2020) European wildfire danger and vulnerability in a changing climate: towards integrating risk dimensions. Technical report by the Joint Research Centre JRC PESETA IV project: Task 9 forest fires. (Publications Office of the European Union: Luxembourg). Available at https://data.europa.eu/doi/10.2760/46951

Curt T, Fréjaville T, Bouillon C (2014) Characterizing pyroregions in south-eastern France. In 'Advances in Forest Fire Research. Chapter 4 – Fire Risk Assessment and Climate Change'. pp. 1093–1101 (Imprensa da Universidade de Coimbra: Coimbra, Portugal.)

Duane A, Brotons L (2018) Synoptic weather conditions and changing fire regimes in a Mediterranean environment. *Agricultural and Forest Meteorology* **253–254**, 190–202. doi:10.1016/J.AGRFORMET.2018.02.014

Dupuy J, Fargeon H, Martin-StPaul N, Pimont F, Ruffault J, Guijarro M, Hernando C, Madrigal J, Fernandes P (2020) Climate change impact on future wildfire danger and activity in southern Europe: a review. *Annals of Forest Science* **77**, 35. doi:10.1007/S13595-020-00933-5

Earl N, Simmonds I (2018) Spatial and temporal variability and trends in 2001–2016 global fire activity. *Journal of Geophysical Research, D, Atmospheres* **123**, 2524–2536. doi:10.1002/2017JD027749

Erni S, Wang X, Taylor S, Boulanger Y, Swystun T, Flannigan M, Parisien M-A (2019) Developing a two-level fire regime zonation system for Canada. *Canadian Journal of Forest Research* **50**, 259–273. doi:10.1139/CJFR-2019-0191

European Union (2018) Copernicus Land Monitoring Service 2018. European Environmental Agency (EEA). Available at https://land.copernicus.eu/

Fargeon H, Pimont F, Martin-StPaul N, De Caceres M, Ruffault J, Barbero R, Dupuy J-L (2020) Projections of fire danger under climate change over France: where do the greatest uncertainties lie? *Climatic Change* **160**, 479–493. doi:10.1007/S10584-019-02629-W

Fernandes PM, Loureiro C, Guiomar N, Pezzatti GB, Manso FT, Lopes L (2014) The dynamics and drivers of fuel and fire in the Portuguese public forest. *Journal of Environmental Management* **146**, 373–382. doi:10.1016/J.JENVMAN.2014.07.049

Fernandes PMA, Santos J, Castedo-Dorado F, Almeida R (2021) Fire from the sky in the Anthropocene. *Fire* **4**, 13. doi:10.3390/FIRE4010013

Flannigan MD, Logan KA, Amiro BD, Skinner WR, Stocks BJ (2005) Future area burned in Canada. *Climatic Change* **72**, 1–16. doi:10.1007/S10584-005-5935-Y

Forzieri G, Girardello M, Ceccherini G, Spinoni J, Feyen L, Hartmann H, Beck PSA, Camps-Valls G, Chirici G, Mauri A, Cescatti A (2021) Emergent vulnerability to climate-driven disturbances in European forests. *Nature Communications* **12**, 1081. doi:10.1038/S41467-021-21399-7

Fréjaville T, Curt T (2015) Spatiotemporal patterns of changes in fire regime and climate: defining the pyroclimates of south-eastern France (Mediterranean Basin). *Climatic Change* **129**, 239–251. doi:10.1007/S10584-015-1332-3

Fréjaville T, Curt T (2017) Seasonal changes in the human alteration of fire regimes beyond the climate forcing. *Environmental Research Letters* **12**, 035006. doi:10.1088/1748-9326/AA5D23

Galizia LF, Curt T, Barbero R, Rodrigues M (2021) Assessing the accuracy of remotely sensed fire datasets across the southwestern Mediterranean Basin. *Natural Hazards and Earth System Sciences* **21**, 73–86. doi:10.5194/NHESS-21-73-2021

Ganteaume A, Camia A, Jappiot M, San-Miguel-Ayanz J, Long-Fournel M, Lampin C (2013) A review of the main driving factors of forest fire ignition over Europe. *Environmental Management* **51**, 651–662. doi:10.1007/S00267-012-9961-Z

Giglio L, Boschetti L, Roy D, Hoffmann AA, Humber M, Hall JV (2018) 'Collection 6 MODIS Burned Area Product User's Guide Version 1.2.' (NASA EOSDIS Land Processes DAAC: Sioux Falls, SD)

Harris RMB, Remenyi TA, Williamson GJ, Bindoff NL, Bowman DMJS (2016) Climate–vegetation–fire interactions and feedbacks: trivial detail or major barrier to projecting the future of the Earth system? *Wiley Interdisciplinary Reviews: Climate Change* **7**, 910–931. doi:10.1002/WCC.428

Jiménez-Ruano A, Rodrigues Mimbrero M, Jolly WM, de la Riva Fernández J (2019) The role of short-term weather conditions in temporal dynamics of fire regime features in mainland Spain. *Journal of Environmental Management* **241**, 575–586. doi:10.1016/J.JENVMAN.2018.09.107

Jiménez-Ruano A, de la Riva Fernández J, Rodrigues M (2020) Fire regime dynamics in mainland Spain. Part 2: A near-future prospective of fire activity. *The Science of the Total Environment* **705**, 135842. doi:10.1016/J.SCITOTENV.2019.135842

Johnston LM, Wang X, Erni S, Taylor SW, McFayden CB, Oliver JA, Stockdale C, Christianson A, Boulanger Y, Gauthier S, Arseneault D, Wotton BM, Parisien M-A, Flannigan MD (2020) Wildland fire risk research in Canada. *Environmental Reviews* **28**, 164–186. doi:10.1139/ER-2019-0046

Krebs P, Pezzatti GB, Mazzoleni S, Talbot LM, Conedera M (2010) Fire regime: history and definition of a key concept in disturbance ecology. *Theory in Biosciences* **129**, 53–69. doi:10.1007/S12064-010-0082-Z

Kreft H, Jetz W (2010) A framework for delineating biogeographical regions based on species distributions: global quantitative biogeographical regionalizations. *Journal of Biogeography* **37**, 2029–2053. doi:10.1111/J.1365-2699.2010.02375.X

Krikken F, Lehner F, Haustein K, Drobyshev I, van Oldenborgh GJ (2021) Attribution of the role of climate change in the forest fires in Sweden 2018. *Natural Hazards and Earth System Sciences* **21**, 2169–2179. doi:10.5194/nhess-21-2169-2021

Laurent P, Mouillot F, Yue C, Ciais P, Moreno MV, Nogueira JMP (2018) FRY, a global database of fire patch functional traits derived from space-borne burned area products. *Scientific Data* **5**, 180132. doi:10.1038/SDATA.2018.132

Moreira F, Ascoli D, Safford H, Adams MA, Moreno JM, Pereira JMC, Catry FX, Armesto J, Bond W, González ME, Curt T, Koutsias N, McCaw L, Price O, Pausas JG, Rigolot E, Stephens S, Tavsanoglu C, Vallejo VR, Van Wilgen BW, Xanthopoulos G, Fernandes PM (2020) Wildfire management in Mediterranean-type regions: paradigm change needed. *Environmental Research Letters* **15**, 011001. doi:10.1088/1748-9326/AB541E

Moreno MV, Chuvieco E (2013) Characterising fire regimes in Spain from fire statistics. *International Journal of Wildland Fire* **22**, 296–305. doi:10.1071/WF12061

Morgan P, Hardy CC, Swetnam TW, Rollins MG, Long DG (2001) Mapping fire regimes across time and space: understanding coarse and fine-scale fire patterns. *International Journal of Wildland Fire* **10**, 329–342. doi:10.1071/WF01032

Oliveira S, Moreira F, Boca R, San-Miguel-Ayanz J, Pereira JMC (2014) Assessment of fire selectivity in relation to land cover and topography: a comparison between Southern European countries. *International Journal of Wildland Fire* **23**, 620–630. doi:10.1071/WF12053

Parisien M-A, Moritz MA (2009) Environmental controls on the distribution of wildfire at multiple spatial scales. *Ecological Monographs* **79**, 127–154. doi:10.1890/07-1289.1

Parisien M-A, Parks SA, Krawchuk MA, Little JM, Flannigan MD, Gowman LM, Moritz MA (2014) An analysis of controls on fire activity in boreal Canada: comparing models built with different temporal resolutions. *Ecological Applications* **24**, 1341–1356. doi:10.1890/13-1477.1

Pausas JG, Keeley JE (2021) Wildfires and global change. *Frontiers in Ecology and the Environment* **19**, 387–395. doi:10.1002/FEE.2359

Pausas JG, Paula S (2012) Fuel shapes the fire-climate relationship: evidence from Mediterranean ecosystems: Fuel shapes the fire–climate relationship. *Global Ecology and Biogeography* **21**, 1074–1082. doi:10.1111/J.1466-8238.2012.00769.X

Pausas JG, Ribeiro E (2013) The global fire-productivity relationship: fire and productivity. *Global Ecology and Biogeography* **22**, 728–736. doi:10.1111/GEB.12043

Pellizzaro G, Cesaraccio C, Duce P, Ventura A, Zara P (2007) Relationships between seasonal patterns of live fuel moisture and meteorological drought indices for Mediterranean shrubland species. *International Journal of Wildland Fire* **16**, 232–241. doi:10.1071/WF06081

Pimont F, Fargeon H, Opitz T, Ruffault J, Barbero R, Martin-StPaul N, Rigolot E, Riviére M, Dupuy J (2021) Prediction of regional wildfire activity in the probabilistic Bayesian framework of Firelihood. *Ecological Applications* **31**, e02316. doi:10.1002/EAP.2316

Pinto GASJ, Rousseu F, Niklasson M, Drobyshev I (2020) Effects of human-related and biotic landscape features on the occurrence and size of modern forest fires in Sweden. *Agricultural and Forest Meteorology* **291**, 108084. doi:10.1016/J.AGRFORMET.2020.108084

Ripley BD (1996) 'Pattern Recognition and Neural Networks.' (Cambridge University Press: Cambridge)

Rodrigues M, Trigo RM, Vega-García C, Cardil A (2020*a*) Identifying large fire weather typologies in the Iberian Peninsula. *Agricultural and Forest Meteorology* **280**, 107789. doi:10.1016/J.AGRFORMET.2019.107789

Rodrigues M, Jiménez-Ruano A, de la Riva J (2020*b*) Fire regime dynamics in mainland Spain. Part 1: drivers of change. *The Science of the Total Environment* **721**, 135841. doi:10.1016/J.SCITOTENV.2019.135841

Rodrigues M, Mariani M, Russo A, Salis M, Galizia L, Cardil A (2021) Spatio-temporal domains of wildfire-prone teleconnection patterns in the Western Mediterranean Basin. *Geophysical Research Letters* **48**, e2021GL094238. doi:10.1029/2021GL094238

Roteta E, Bastarrika A, Padilla M, Storm T, Chuvieco E (2019) Development of a Sentinel-2 burned area algorithm: generation of a small fire database for sub-Saharan Africa. *Remote Sensing of Environment* **222**, 1–17.

Ruffault J, Curt T, Moron V, Trigo RM, Mouillot F, Koutsias N, Pimont F, Martin-StPaul N, Barbero R, Dupuy J-L, Russo A, Belhadj-Khedher C (2020) Increased likelihood of heat-induced large wildfires in the Mediterranean Basin. *Scientific Reports* **10**, 13790. doi:10.1038/S41598-020-70069-Z

San-Miguel-Ayanz J, de Rigo D, Caudullo G, Durrant TH, Mauri A (2016) 'European Atlas of Forest Tree Species.' (Publication Office of the European Union: Luxembourg.)

Silva JMN, Moreno MV, Le Page Y, Oom D, Bistinas I, Pereira JMC (2019) Spatiotemporal trends of area burnt in the Iberian Peninsula, 1975–2013. *Regional Environmental Change* **19**, 515–527. doi:10.1007/S10113-018-1415-6

Sjöström J, Plathner FV, Granström A (2019) Wildfire ignition from forestry machines in boreal Sweden. *International Journal of Wildland Fire* **28**, 666–677. doi:10.1071/WF18229

Sørensen TJ (1948) 'A Method of Establishing Groups of Equal Amplitude in Plant Sociology Based on Similarity of Species Content and its Application to Analyses of the Vegetation on Danish Commons.' (Munksgaard: Copenhagen, Denmark)

Taylor SW (2020) Atmospheric cascades shape wildfire activity and fire management decision spaces across scales – a conceptual framework for fire prediction. *Frontiers in Environmental Science* **8**, 527278. doi:10.3389/FENVS.2020.527278

Turco M, Bedia J, Liberto FD, Fiorucci P, von Hardenberg J, Koutsias N, Llasat M-C, Xystrakis F, Provenzale A (2016) Decreasing fires in Mediterranean Europe. *PLoS One* **11**, e0150663. doi:10.1371/journal.pone.0150663

Turco M, von Hardenberg J, AghaKouchak A, Llasat MC, Provenzale A, Trigo RM (2017) On the key role of droughts in the dynamics of summer fires in Mediterranean Europe. *Scientific Reports* **7**, 81. doi:10.1038/S41598-017-00116-9

Turco M, Herrera S, Tourigny E, Chuvieco E, Provenzale A (2019) A comparison of remotely-sensed and inventory datasets for burned area in Mediterranean Europe. *International Journal of Applied Earth Observation and Geoinformation* **82**, 101887. doi:10.1016/J.JAG.2019.05.020

Van Wagner CE (1987) Development and structure of the Canadian Forest Fire Weather Index System. Canadian Forestry Service, Forestry Technical Report 35 (Ottawa).

Venäläinen A, Korhonen N, Koutsias N, Xystrakis F, Urbieta IR, Moreno JM (2013) Temporal variations and change of forest fire danger in Europe in 1960–2012. *Natural Hazards and Earth System Sciences – Discussions* **1**, 6291–6326. doi:10.5194/NHESSD-1-6291-2013

Vitolo C, Di Giuseppe F, Barnard C, Coughlan R, San-Miguel-Ayanz J, Libertá G, Krzeminski B (2020) ERA5-based global meteorological wildfire danger maps. *Scientific Data* **7**, 216. doi:10.1038/S41597-020-0554-Z

Wang X, Studens K, Parisien M-A, Taylor SW, Candau J-N, Boulanger Y, Flannigan MD (2020) Projected changes in fire size from daily spread potential in Canada over the 21st century. *Environmental Research Letters* **15**, 104048. doi:10.1088/1748-9326/ABA101

Ward JH (1963) Hierarchical grouping to optimize an objective function. *Journal of the American Statistical Association* **58**, 236–244. doi:10.1080/01621459.1963.10500845

Williams AP, Seager R, Macalady AK, Berkelhammer M, Crimmins MA, Swetnam TW, Trugman AT, Buenning N, Noone D, McDowell NG, Hryniw N, Mora CI, Rahn T (2015) Correlations between components of the water balance and burned area reveal new insights for predicting forest fire area in the southwest United States. *International Journal of Wildland Fire* **24**, 14–26. doi:10.1071/WF14023

Yin S, Wu W, Zhao X, Gong C, Li X, Zhang L (2020) Understanding spatiotemporal patterns of global forest NPP using a data-driven method based on GEE. *PLoS One* **15**, e0230098. doi:10.1371/JOURNAL.PONE.0230098